Imaging Review of Connective Tissue Diseases

Thurl Hugh C. Cledera, MD, and Dyan V. Flores, MD

After completing this educational activity, the radiologist should be better able to describe the pathophysiologic processes, clinical manifestations, and characteristic imaging features of various connective tissue diseases.

Category: Musculoskeletal
Subcategory: Chest
Modality: Multiple

Key Words: Scleroderma, Systemic Lupus Erythematosus, Sjögren Syndrome, Myopathy, Arthritis, Marfan Syndrome, Ehlers Danlos, Connective Tissue Disease, Collagen Vascular Disease

Connective tissue diseases (CTDs) form a group of chronic inflammatory disorders characterized by disturbance in immune mechanisms and defective clearance of apoptotic and immune complexes. Virtually all cells and tissues containing collagen or elastin are affected, resulting in multisystemic derangements and significant morbidity and mortality. Clinical manifestations are nonspecific and may not occur simultaneously, predisposing to a delayed or missed diagnosis. Imaging aids in supporting the diagnosis when diagnostic criteria are not met, determining extent and severity of disease, and monitoring treatment response and complications.

In this article, we briefly review pathogenesis, clinical features, and imaging findings of CTDs usually encountered in clinical practice, emphasizing imaging features that are either common or unique to each CTD (See Supplemental Digital Content 1, published online, http://links.lww.com/CDR/A6).

Scleroderma

Scleroderma (SSc) is a systemic connective tissue disease chiefly characterized by small-vessel vasculopathy, organ fibrosis, and soft tissue calcifications. There are two major types: diffuse cutaneous (DSSc) and limited (LSSc). DSSc is rapidly progressive, with frequent dermal manifestations and involvement of more visceral organs. LSSc, also known as morphea, is confined to the face, arms, and hands, and is less significant radiologically. The classic presentation is a middle-aged female with extreme sensitivity to cold or Raynaud's phenomenon (RP), skin tightening, joint and muscle pain, difficulty swallowing, and shortness of breath.[1] In 2015, the European League Against Rheumatism (EULAR) and the American College of Rheumatology (ACR) updated the diagnostic criteria by incorporating new elements (proximal SSc, sclerodactyly, digital pits, pulmonary fibrosis, RP, and SSc-specific autoantibodies), emphasizing vasculopathy and including the early manifestation of puffy fingers.[2]

The skin is the most commonly involved organ, presenting with thickening, induration, and telangiectasias. It may be clinically assessed using a dedicated scoring system (modified Rodman score), although high-frequency ultrasonography (US) offers an objective alternative that allows differentiation of edema from fibrosis.[1] Both US and MRI are capable of delineating LSSc and excluding underlying myositis. The esophagus is second to the skin in organ involvement.[1] Barium contrast studies are the traditional

Dr. Cledera is a Resident, Institute of Radiology, St Luke's Medical Center Global City, Taguig, Metro Manila, Philippines; and Dr. Flores is a Musculoskeletal Radiologist, Department of Medical Imaging, The Ottawa Hospital, University of Ottawa, 501 Smyth Rd, Ottawa, ON K1H 8L6, Canada; E-mail: dflores@toh.ca.

methods of examination and readily reveal loss of esophageal dysmotility, atrophy, and patulous appearance. Because barium contrast can lead to pseudo-obstruction, some institutions prefer CT and MRI to demonstrate a fluid-filled and dilated esophagus.[1] "Hidebound appearance" is characterized by small bowel fibrosis with luminal dilation and longitudinal approximation of the folds of the valvulae conniventes.[3] A jejunal diameter larger than 3 cm, more than seven folds per inch, and preservation of normal fold spacing on a background of bowel dilation are positive signs.[3] Pseudosacculation or asymmetric fibrosis of one side of the bowel wall (usually the antimesenteric side), transient intussusceptions, benign pneumatosis cystoides intestinalis, and delayed motility resulting in fecalization of the small bowel ("small bowel feces sign") can also occur.[3]

Articular symptoms are reported in approximately 10% to 60% of patients at the time of diagnosis, and are frequently the initial manifestation.[4] The hand is the most characteristic site of musculoskeletal (MSK) involvement, usually manifesting with RP, soft tissue thinning, sclerodactyly, digital pits and ulcers, and acro-osteolysis.[1] Acro-osteolysis tends to involve the palmar surface initially of the terminal phalangeal tuft, but can progress to the appearance of a pencil tip.[1] Erosions can occur in the metacarpophalangeal (MCP) and distal interphalangeal (DIP) joints; a distinctive carpometacarpal erosion with associated radial subluxation has also been reported.[1]

SSc-related interstitial lung disease (SSc-ILD) is the most common pulmonary manifestation, and along with pulmonary hypertension (PH), is the leading cause of mortality in SSc.[5] Imaging and histopathologic pattern consistent with nonspecific interstitial pneumonia (NSIP) rather than usual interstitial pneumonia (UIP) is typical for SSc.[5] Similar to UIP, NSIP findings on high-resolution CT (HRCT) include reticular interstitial markings predominantly involving the posterior basal aspects of the lower lobes. Contrary to UIP, NSIP is characterized by ground-glass opacities with more frequent subpleural sparing and lesser prevalence of traction bronchiectasis (Figure 1).

Systemic Lupus Erythematosus

Systemic lupus erythematosus (SLE) is a chronic, progressive, autoimmune disorder characterized by inflammation, immune complex deposition, and vasculopathy. The peak age of onset is the second to fourth decades of life with a female predisposition.[6] In 2019, the EULAR-ACR formulated new diagnostic criteria for SLE.[7] Among the changes include placing greater significance on positive antinuclear antibodies as an entry criterion, attribution to SLE only if there is no likely alternative explanation, and emphasizing histologically evident lupus nephritis in the diagnosis of SLE.[7]

Apart from pleural disease that occurs in 21% of patients, other respiratory manifestations are very uncommon in SLE, occurring in fewer than 4% of patients.[8] Pleural effusions are the most common respiratory manifestation and are bilateral in approximately half of these patients.[6] An isolated pleural effusion is a nonspecific finding but may suggest autoimmune disease when chronic.[6] The risk of pulmonary infection is three times higher in patients with SLE than in the general population.[6] Pneumonia can be atypical and advanced at the time of initial presentation. Of particular note is *Nocardia* infection, which is slightly higher in prevalence for SLE patients than in the general population.[9]
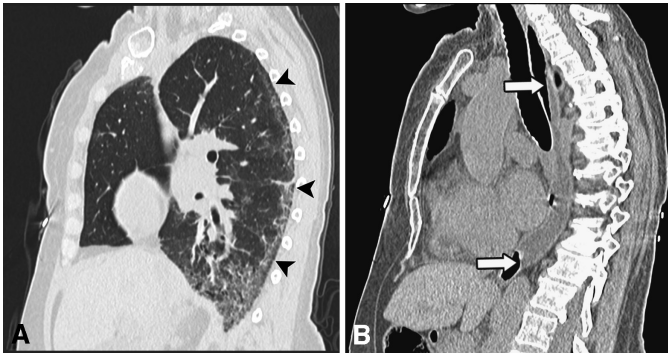

Figure 1. Lung and mediastinum in SSc. Sagittal chest CT images using lung window (*A*) and mediastinal window (*B*) settings in a 62-year-old woman diagnosed with SSc show ground-glass densities in the lower lung zones with subpleural sparing (*arrowheads*). The esophagus is also patulous in appearance with stasis of fluid (*arrows*).

Other imaging findings include pulmonary infiltrates, pulmonary alveolar hemorrhage, ILD, pulmonary embolism secondary to circulating autoantibodies, and PH. Valvular disease is the most common cardiac manifestation of SLE. It occurs in up to 75% of SLE patients and can range from valve leaflet thickening to Libman-Sacks endocarditis.[6] The latter is a characteristic sterile lesion of the valves and subendocardium, which can be clinically silent but can precipitate the risk of embolism. Abnormalities of the pericardium, myocardium, and coronary arteries may also be seen. Echocardiography and advanced cine cardiac MR techniques allow noninvasive definition of subtle wall motion abnormality but may not always be reliable.[6] Lupus nephritis occurs in 50% of SLE patients.[6] Imaging findings are generally nonspecific and similar to those in other causes of renal disease. At US, the kidneys are hyperechoic and small, although the size of the kidney generally depends on duration of renal involvement.[6] Over 80% of SLE patients have bilateral, symmetric, nonerosive, nondeforming polyarthritis affecting the small joints of the hands, wrists, knees, and shoulders.[6] Ulnar deviation of the fingers and toes with MCP or metatarsophalangeal (MTP) joint subluxation or Jaccoud arthropathy can occur and lead to irreversible deformities and contractures (Figure 2). Antiphospholipid antibody syndrome (APL-AB) can be either primary or secondary. Patients with APL-AB secondary to SLE present with recurrent strokes, dural venous sinus thrombosis, Budd-Chiari syndrome, ischemic bowel, miscarriages, and recurrent pulmonary embolism.[6] Diagnosis is made by a combination of clinical and laboratory criteria.[10]

In SLE, pleural effusions are the most common respiratory manifestation and are bilateral in approximately half of patients.

Sjögren Syndrome

Sjögren syndrome (SjS) is a lymphocytic infiltration or "autoimmune epithelitis" primarily of the salivary and lacrimal glands. The incidence of SjS ranges between 3 and 11 cases per 100,000 individuals, although this is likely underestimated given that asymptomatic cases are not diagnosed.[11] There is a 10:1 female predilection and can occur at all ages,

Figure 2. Lupus hands. Ball-catcher radiograph of both hands in a 52-year-old woman with longstanding SLE shows ulnar-sided MCP joint deviation in the second and third digits bilaterally and fourth and fifth digits of the right hand (*dashed circles*). Note the absence of erosive changes in contrast to other MCP joint arthropathies.

mainly between 30 and 50 years of age.[11] The cardinal features are keratoconjunctivitis sicca (xerophthalmia); xerostomia or dryness of the mucous membrane of the mouth (xerostomia); and bilateral parotid enlargement. SjS can be primary when it occurs by itself or secondary when it coincides with another CTD. Secondary SjS is diagnosed when someone with an established SSc, rheumatoid arthritis (RA), or SLE develops extreme dryness of the eyes and mouth or sicca symptoms. The diagnostic criterion was updated by the EULAR-ACR most recently in 2016, although this was developed mainly for patients entering clinical trials and not for clinical diagnosis.[12]

The thorax is a commonly affected site. Airway abnormalities, interstitial pneumonias, lymphoid hyperplasia, mediastinal lymph node enlargement, thymic lymphoid hyperplasia, and thymic cysts can occur.[13] Air cysts are characteristic of primary SjS and present on HRCT as well-defined, round, thin-walled airspaces that have a tendency to involve the peribronchovascular regions (Figure 3).[13] It is important to monitor for potential infections, acute exacerbation of interstitial pneumonia, and the possibility of concomitant malignant lymphoma during interval follow-ups.[13] Aside from the lungs, the salivary glands are another common site of cystic changes. On US, early SSc can present with either normal or enlarged and hyperechoic salivary glands.[14] In advanced disease, atrophy with a multicystic or reticular pattern is more typical.[14] On MR, a heterogeneous appearance on T1- and T2-weighted sequences in late SjS is termed "salt and pepper" or honeycomb appearance (Figure 4).[15] The appearance is attributed to pathologic lymphocytic aggregates causing interlobular fibrosis and decreased signal intensity (pepper) interspersed with multicystic changes (salt).[15]

Idiopathic Inflammatory Myopathies

Idiopathic inflammatory myopathy (IIM) is a group of rare heterogeneous autoimmune disorders with a common clinical
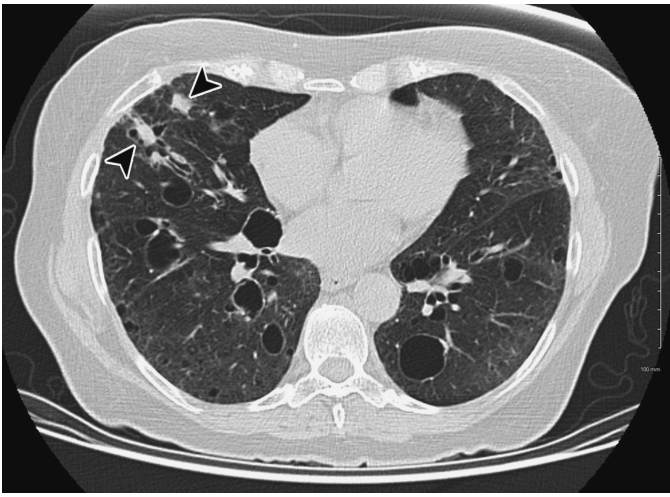
Figure 3. Lymphoid interstitial pneumonia. Axial chest CT in a 75-year-old woman demonstrates multiple cysts in both lungs. There are also peribronchovascular nodules in the right lung (*arrowheads*).

presentation of muscle weakness. There is continuing evolution in the classification criteria of IIM, with the rise of autoantibody testing and increasing importance of clinicoserologic correlation. Imaging is primarily an ancillary tool, allowing assessment of disease progression, monitoring of treatment response, and detection of an optimal biopsy site.

In IIM, large FOV MRI sequences encompassing both upper and lower extremities enable evaluation of disease distribution and severity.

Among the available imaging tools, MRI is the most recognized and established. Large field-of-view (FOV) sequences encompassing both upper and lower extremities enable evaluation of disease distribution and severity. A combination of T1-W (for atrophy and fatty infiltration) and fluid-sensitive sequences (to detect active inflammation) is usually performed. Short-tau inversion recovery is preferred by some institutions, as it provides homogeneous fat suppression over large FOV sequences.[15] Advanced quantitative models are now being tested although data on clinical applicability remain limited.[16] The criterion for diagnosis originated by Bohan and Peter in 1975 has since been modified and expanded into various subtypes based on clinical features, laboratory and serologic findings, and better defined muscle
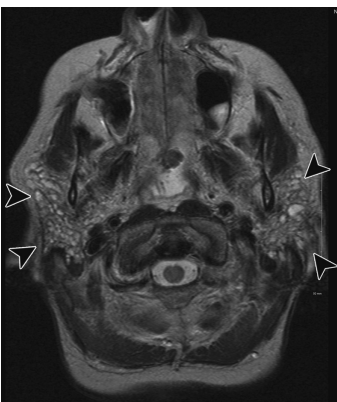

Figure 4. Parotid glands in Sjögren syndrome. Axial T2-weighted image of the brain in a 65-year-old woman with chronic headaches shows incidental findings of multicystic appearance of both parotid glands (*arrowheads*). CT of the brain done earlier the same day (not shown) also revealed sparsely distributed calcifications within the glands.

Figure 5. Dermatomyositis. AP radiograph of the abdomen and pelvis in a 47-year-old woman demonstrates diffuse lacy reticular calcifications.

biopsy standards.[17,18] We discuss two of the more well-recognized subtypes: dermatomyositis (DM) and inclusion body myositis (IBM).

In recent iterations of IIM classification, polymyositis (PM) is a diagnosis of exclusion. It represents fewer than 5% of patients and will likely cease to exist upon further studies on autoantibodies. Cases previously diagnosed as PM using the Bohan and Peter classification were potentially IBM or other subtypes.

DM has two types: juvenile DM, which affects children and tends to be more severe; and adult DM, which frequently occurs in those around the age of 50 years. Gottron's papules (flat red rashes on the dorsal surfaces of the hands and elbows), shawl sign (diffuse flat red rash along the upper back, shoulders, and back of the neck), and a heliotrope rash (violaceous rash typically in the upper eyelids and other sun-exposed areas) comprise the constellation of dermal manifestations; however, the presence of rash is not specific for DM.[19] A considerable number of patients with serology and extracutaneous features that are more consistent with a non-DM subtype will eventually develop cutaneous manifestations.[18] Among imaging features, soft tissue calcifications are a classic finding and present with four patterns: superficial nodular (skin/subcutaneous), lacy reticular (subcutaneous), deep tumorous (intramuscular), and deep linear or sheet-like (fascial/peritendinous) (Figure 5).[19,20] MRI findings reflect the pattern of muscle weakness: bilateral symmetric, proximal greater than distal, and lower greater than upper extremity.[17]

IBM is a rare inflammatory myopathy typically involving males and patients older than 50 years.[17] IBM patients do not develop a DM rash or other overlapping features. Several diagnostic criteria have been devised for IBM incorporating both clinical and histologic features although serology has yet to be incorporated into the criteria.[17] On MRI, muscle involvement is bilateral and symmetric with volume loss and fatty infiltration rather than edema. There is a predilection for the anterior compartment of the thigh, posterior compartment of the calf, and anterior compartment of the forearm (Figure 6).[21] Within the thigh anterior compartment, the rectus femoris is relatively spared, whereas the vastus lateralis is the most severely involved.[21] The "undulating fascia" sign refers to severe atrophy and fatty infiltration of the vastus intermedius and lateralis.[22] In the lower leg, the posterior compartment is much more frequently involved than the anterior or lateral compartments; the medial gastrocnemius is more predisposed compared with its lateral counterpart.[22] In the volar aspect of the forearm, involvement of flexor digitorum profundus with complete sparing of flexor carpi ulnaris
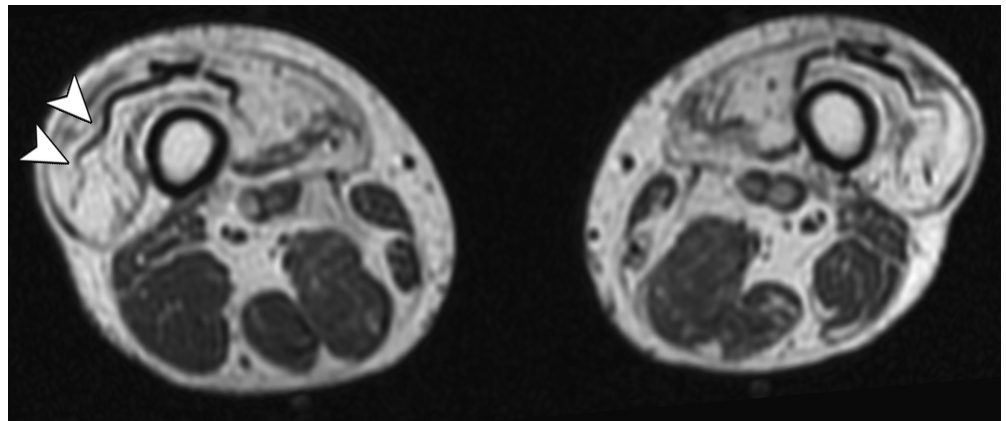
Figure 6. Inclusion body myositis. Axial T1-weighted MR image of the lower extremities in a 63-year-old man demonstrates atrophy primarily involving the anterior compartments of both thighs. The undulating fascia sign is seen in the right (*arrowheads*).

has been shown to be an excellent discriminator of IBM from other inflammatory myopathies and their subtypes.[22]

Mixed Connective Tissue Disease

Mixed connective tissue disease (MCTD) is a systemic autoimmune disease characterized by overlapping features between at least two of the following: SLE, SSc, DM/PM, and RA.[23] It has a female predilection and occurs in 3.8 per 100,000 adults.[23] It can affect various organ systems with pulmonary and MSK being two of the most vital systems affected.[23] Pulmonary complications occur in 85% of cases and include interstitial changes, pleural effusions, and pleural thickening. MCTD arthropathy manifests with RA-like changes involving both small and large joints.[19] Other MSK findings include soft tissue calcifications, sclerodactyly, and acro-osteolysis.

Seronegative CTDs

Ankylosing spondylitis (AS), psoriatic arthritis (PsA), reactive arthritis (RcA), and enteropathic arthritis (EA) form a group of diseases involving patients with negative rheumatoid factor, hence seronegative. Imaging findings for these entities may be similar to each other but with different patterns of distribution.

Imaging findings for seronegative spondyloarthropathies may be similar to each other but with different patterns of distribution.

AS is a spondyloarthropathy-producing bony fusion (ankylosis) of the spine and sacroiliac joints. Multiple genes contribute to its pathogenesis although *HLA-B27* demonstrates the strongest association. The most well-recognized imaging features are found in the axial skeleton. The hallmark of AS is bilateral and symmetric sacroiliitis. Radiographs depict subchondral irregularity, erosions, and sclerosis. In contrast to radiographs, CT and MRI can detect subchondral edema in early disease and soft tissue changes such as synovitis. Spinal abnormalities primarily involve the discovertebral unit: erosions in the vertebral body corners (Romanus lesions); thin and flowing syndesmophytes (bamboo spine), bone repair (shiny corners); and discal calcification and ballooning. Apophyseal joint involvement shows ankylosis, ligamentous calcifications, and edema.[24] On frontal radiographs, a single central radiodense line related to ossified posterior interspinous

ligament secondary to enthesitis is referred to as the "dagger sign"; the addition of lateral vertical lines on either side representing ossified apophyseal joint capsules makes up the "trolley-track sign."[4] Complications from abnormalities in the axial skeleton predispose to formation of pseudoarthrosis and fractures (Figure 7). The most common extra-articular manifestation is acute anterior uveitis.[25] Cardiac abnormalities are also seen in 10% to 30% of cases and include aortic valve abnormalities, conduction disturbances, and cardiac blocks.[25] ILD in AS is characterized by apical fibrosis, bronchiectasis, and bullous changes (Figure 8).[25]

PsA is a chronic inflammatory disease affecting joints and entheses of the axial and appendicular skeleton. It affects up to 40% of patients with psoriasis and occurs in 10% to 15% of patients with the skin exanthem.[24,26] Its age of onset is before 40 years, with males and females equally affected.[24,26] Clinical patterns include oligoarticular (fewer than four joints, asymmetric), polyarticular (more than five joints, symmetric, RA-like), distal (exclusive to the distal interphalangeal joints or DIP joints of the hands), and axial skeleton (spine and sacroiliac joints). Key imaging features are seen in the appendicular skeleton and include destructive changes of DIP joints of the hands and feet, acro-osteolysis, ankylosis, and periosteal bone formation. The gull-wing appearance may be seen in PsA, but also in erosive osteoarthritis (OA) and RA (Figure 9). Arthritis mutilans also termed as telescoping of digits or opera glass hand is a destructive subtype. It is not specific to psoriasis and may be seen in advanced RA and erosive OA. In contrast to the thin and flowing
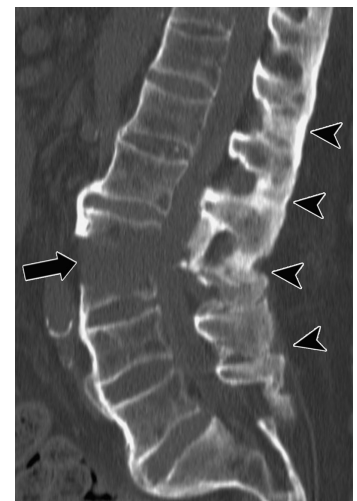

Figure 7. Ankylosing spondylitis. Reconstructed sagittal CT image in a 68-year-old man demonstrates a fracture of the L3 vertebral body (*arrow*). There is dense ossification of the interspinous ligaments (*arrowheads*).

Figure 8. Bullous lung disease in AS. Coronal chest CT image in a 69-year-old man shows large bulla (*arrows*) with areas of fibrosis (*arrowheads*) in the left upper lung.

Figure 10. Crohn's disease. Coronal CT image of the abdomen (*A*) in a 55-year-old woman with Crohn's disease and recent right upper quadrant pain shows the loss of normal colonic haustrations with stasis of fluid in the ascending colon (*arrows*). Axial CT image (*B*) demonstrates erosions and sclerosis in both sacroiliac joints (*arrowheads*) consistent with enteropathic sacroiliitis.

syndesmophytes in AS, syndesmophytes in PsA can be asymmetric and bulky, mimicking diffuse idiopathic skeletal hyperostosis.[25] The most common extraosseous findings are IBM and uveitis/conjunctivitis.

Reiter's or Fiessinger-Leroy syndromes were the historical names for RcA.[27] Over the years, the term RcA has become the appropriate terminology for this disease process regardless of whether or not the classic triad of uveitis or conjunctivitis, urethritis, and arthritis is present.[27] It is a sterile arthritis arising from a previous gastrointestinal (GIT) (*Salmonella, Shigella, Campylobacter*, and *Yersinia*) or genitourinary (*Chlamydia trachomatis*) infection.[27] Ocular manifestations occur in up to 96% of patients and include conjunctivitis and anterior uveitis.[28] Arthropathy occurs in a symmetric oligoarthritic pattern primarily involving the large joints of the lower extremities. In the appendicular skeleton, the knee, ankle, and foot are preferentially and most severely affected, contrary to PsA, which has a predilection for the upper extremities.[26]

EA is a spondyloarthritis associated with chronic inflammatory bowel disease (IBM) (Crohn's and ulcerative colitis) or other GIT abnormalities (Whipple's disease, celiac sprue, and intestinal bypass surgery). Arthritis is the most common extraintestinal manifestation and occurs in up to 20% of patients with inflammatory bowel disease.[26] It occurs in two
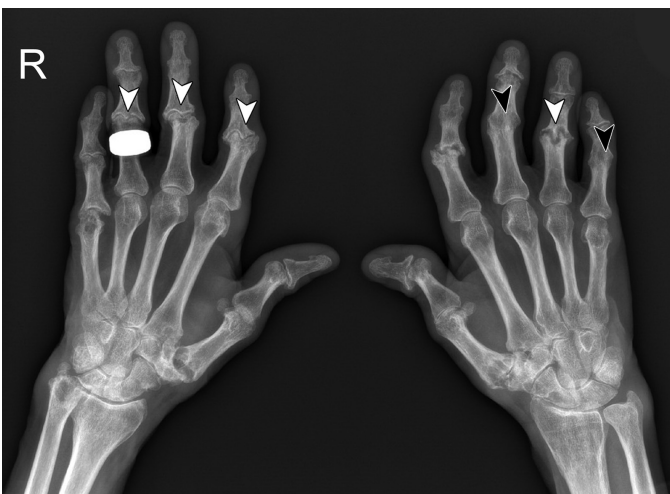

Figure 9. Gull-wing appearance. AP radiograph of both hands in a 73-year-old man show central erosions in the proximal interphalangeal (PIP) joints bilaterally producing seagull erosions or sawtooth appearance (*white arrowheads*). The third and fifth PIP joints of the left hand are completely fused (*black arrowheads*). Scattered erosive changes are also seen in the wrist.
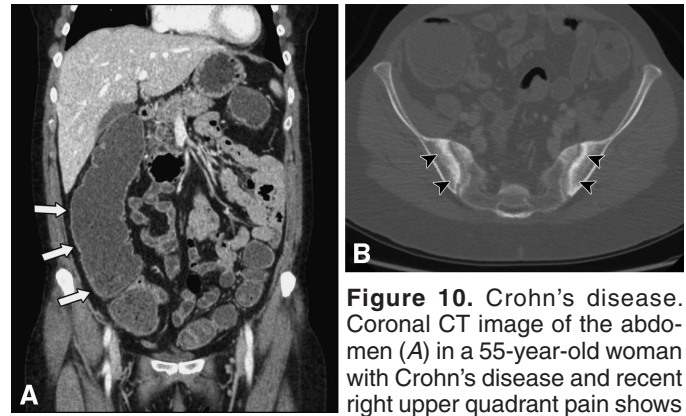
forms. The first form is a nondestructive and often transient peripheral arthritis, which usually involves the knees, ankles, elbows, and wrists in a bilateral and symmetric fashion. The severity parallels the progression of the underlying bowel disease.[26] The second form manifests with spondylitis and/or sacroiliitis, which may occur before the onset of bowel manifestations (Figure 10).[26] Unlike the first form, the severity of the spondylitis and sacroiliitis progresses independent of the course of bowel disease.[26]

Hereditary CTDs

Marfan syndrome (MFS) is a hereditary autosomal disease, with an estimated incidence of two to three per 10,000 individuals.[29] Sporadic mutations occur although mutations of the fibrillin-1 protein (*FBN1*) gene account for 95% of cases.[29] Diagnosis is based on the revised Ghent classification of 2010, which gives more weight to aortic root aneurysm and ectopia lentis.[30] Aortic dissection, congestive heart failure, and cardiac valve disease are the most common causes of death in more than 90% of those affected and, thus, the primary causes of reduction in life expectancy. Annuloaortic ectasia, especially with dilatation of the aortic root, is found in 60% to 80% of adults with MFS.[31]

Dilatation of the aortic root is the leading cause of aortic valve insufficiency in MFS and may progress to aortic root dissection or rupture.[31] The diameters of the dilated ascending aorta, sinotubular junction, and aortic root are clearly demonstrated on multiplanar CT images obtained with three-dimensional reconstruction techniques.[31] Dilatation of the main pulmonary artery is also one of the established criteria for the diagnosis of MFS. Like dilatation of the ascending aorta, it occurs predominantly in the root. The upper limits of a normal main pulmonary artery diameter at the root and at the level of bifurcation are 34.8 and 28.0 mm, respectively.[31]

Scoliosis occurs in approximately 62% of patients with MFS. In contrast to idiopathic scoliosis, MFS scoliosis is commonly seen in younger patients.[31] The Lippman-Cobb method is widely used to measure the degree of scoliotic curvature on standing AP and lateral radiographs of the spine. CT and MR imaging are helpful in evaluating bone structure, abnormalities of the spinal cord, and nerve roots before treatment planning.[31] Approximately 66% of patients with MFS have either pectus

excavatum or pectus carinatum due to longitudinal overgrowth of the ribs.[31] The severity of pectus excavatum is determined by the pectus index obtained on CT images. It is calculated by dividing the width of the chest wall at its widest point by the distance between the posterior surface of the sternum and the anterior surface of the spine. A pectus index greater than 3.25 is an indication for surgery.[31]

Arachnodactyly or "long slender fingers" is another characteristic feature of MFS. Radiographs provide an objective parameter for confirming the presence of disproportionate metacarpal length.[31] To obtain the metacarpal index, the total length (in millimeters) of the second, third, fourth, and fifth metacarpals is divided by the total width of the metacarpals at their exact midpoints. An index between 8.4 and 9.4 is considered abnormal.[31]

Ehlers-Danlos syndromes are an inherited heterogeneous group of CTDs characterized by abnormal collagen synthesis affecting skin, ligaments, joints, blood vessels, and other organs. The original Berlin classification of 1988 listing 11 subtypes defined by Roman numerals has evolved over the years. With the advent of advanced sequencing techniques, mutations have been identified in an array of new genes; the current classification recognizes 13 subtypes.[32] The majority of patients have a bleeding diathesis, which is seen in all subtypes.[33] Ehlers-Danlos syndrome type IV (vascular) has the worst prognosis because of its association with severe and often fatal rupture of the bowel, other organs, and large arteries.[33] Imaging findings reflect the pathogenesis of excessive tissue fragility of arteries and include aneurysms, dissection, rupture, and fistula formation.[33] The abdominal visceral arteries, abdominal aorta, and lower limb are typically involved although the proximal branches of the thoracic aorta and cerebral arteries may also be affected.[33]

Conclusion

There is a plethora of clinical, laboratory, and imaging findings in CTDs making diagnosis daunting for the radiologist and clinician. Increased understanding of the basic pathogenesis along with knowledge of the common and characteristic imaging findings can aid in radiologic detection and interpretation, thereby preventing delays in diagnosis, guiding treatment, and optimizing outcomes.

References

1. Chapin R, Hant FN. Imaging of scleroderma. *Rheum Dis Clin North Am*. 2013;39(3):515-546.
2. Johnson SR. New ACR EULAR guidelines for systemic sclerosis classification. *Curr Rheumatol Rep*. 2015;17(5):32.
3. Levine MS, Rubesin SE, Laufer I. Pattern approach for diseases of mesenteric small bowel on barium studies. *Radiology*. 2008;249(2):445-460.
4. Resnick D. *Diagnosis of Bone and Joint Disorders*. Vol 2. 4th ed. Philadelphia, PA: WB Saunders; 2002.
5. Strollo D, Goldin J. Imaging lung disease in systemic sclerosis. *Curr Rheumatol Rep*. 2010;12(2):156-161.
6. Lalani TA, Kanne JP, Hatfield GA, et al. Imaging findings in systemic lupus erythematosus. *Radioggraphics*. 2004;24(4):1069-1086.
7. Aringer M. EULAR/ACR classification criteria for SLE. *Semin Arthritis Rheum*. 2019;49(3):S14-S17.
8. Narváez J, Borrell H, Sánchez-Alonso F, et al. Primary respiratory disease in patients with systemic lupus erythematosus: Data from the Spanish Rheumatology Society Lupus Registry (RELESSER) cohort. *Arthritis Res Ther*. 2018;20(1):280.
9. Mok CC, Lau CS. Pathogenesis of systemic lupus erythematosus. *J Clin Pathol*. 2003;56(7):481-490.
10. Gardiner C, Hills J, MacHin SJ, et al. Diagnosis of antiphospholipid syndrome in routine clinical practice. *Lupus*. 2013;22(1):18-25.
11. Brito-Zerón P, Baldini C, Bootsma H, et al. Sjögren syndrome. *Nat Rev Dis Primers*. 2016;2:16047.
12. Shiboski CH, Shiboski SC, Seror R, et al. 2016 American College of Rheumatology/European League Against Rheumatism Classification Criteria for Primary Sjögren's Syndrome: A Consensus and Data-Driven Methodology Involving Three International Patient Cohorts. *Arthritis Rheumatol*. 2017;69(1):35-45.
13. Egashira R, Kondo T, Hirai T, et al. CT findings of thoracic manifestations of primary Sjögren syndrome: radiologic-pathologic correlation. *Radiographics*. 2013;33(7):1933-1949.
14. Ching ASC, Ahuja AT. High-resolution sonography of the submandibular space: anatomy and abnormalities. *AJR Am J Roentgenol*. 2002;179(3):703-708.
15. Delfaut EM, Beltran J, Johnson G, et al. Fat suppression in MR imaging: techniques and pitfalls. *Radiographics*. 1999;19(2):373-382.
16. Farrow M, Biglands JD, Grainger AJ, et al. Quantitative MRI in myositis patients: comparison with healthy volunteers and radiological visual assessment. *Clin Radiol*. 2021;76(1):81.e1-81.e10.
17. Dimachkie MM, Barohn RJ, Amato AA. Idiopathic inflammatory myopathies. *Neurol Clin*. 2014;32(3):595-628.
18. Lundberg IE, Tjärnlund A, Bottai M, et al. 2017 European League Against Rheumatism/American College of Rheumatology classification criteria for adult and juvenile idiopathic inflammatory myopathies and their major subgroups. *Ann Rheum Dis*. 2017;76(12):1955-1964.
19. Jacques T, Sudoł-Szopińska I, Larkman N, et al. Musculoskeletal manifestations of non-RA Connective tissue diseases: scleroderma, systemic lupus erythematosus, Still's disease, dermatomyositis/polymyositis, Sjögren's syndrome, and mixed connective tissue disease. *Semin Musculoskelet Radiol*. 2018;22(2):166-179.
20. Blane CE, White SJ, Braunstein EM, et al. Patterns of calcification in childhood dermatomyositis. *AJR Am J Roentgenol*. 1984;142(2):397-400.
21. Phillips BA, Cala LA, Thickbroom GW, et al. Patterns of muscle involvement in inclusion body myositis: clinical and magnetic resonance imaging study. *Muscle Nerve*. 2001;24(11):1526-1534.
22. Guimaraes JB, Zanoteli E, Link TM, et al. Sporadic inclusion body myositis: MRI findings and correlation with clinical and functional parameters. *AJR Am J Roentgenol*. 2017;209(6):1340-1347.
23. Tani C, Carli L, Vagnani S, et al. The diagnosis and classification of mixed connective tissue disease. *J Autoimmun*. 2014;48-49:46-49.
24. Mattar M, Salonen D, Inman RD. Imaging of spondyloarthropathies. *Rheum Dis Clin North Am*. 2013;39(3):645-667.
25. El Maghraoui A. Extra-articular manifestations of ankylosing spondylitis: prevalence, characteristics and therapeutic implications. *Eur J Intern Med*. 2011;22(6):554-560.
26. Soldatos T, Pezeshk P, Ezzati F, et al. Cross-sectional imaging of adult crystal and inflammatory arthropathies. *Skelet Radiol*. 2016;45(9):1173-1191.
27. Carter JD, Hudson AP. Reactive arthritis: clinical aspects and medical management. *Rheum Dis Clin North Am*. 2009;35(1):21-44.
28. Kemeny-Beke A, Szodoray P. Ocular manifestations of rheumatic diseases. *Int Ophthalmol*. 2020;40(2):503-510.
29. Meester JAN, Verstraeten A, Schepers D, et al. Differences in manifestations of Marfan syndrome, Ehlers-Danlos syndrome, and Loeys-Dietz syndrome. *Ann Cardiothorac Surg*. 2017;6(6):582-594.
30. Faivre L, Collod-Beroud G, Adès L, et al. The new Ghent criteria for Marfan syndrome: What do they change? *Clin Genet*. 2012;81(5):433-442.
31. Ha HI, Seo JB, Lee SH, et al. Imaging of Marfan syndrome: multisystemic manifestations. *Radiographics*. 2007;27(4):989-1004.
32. Malfait F, Francomano C, Byers P, et al. The 2017 international classification of the Ehlers-Danlos syndromes. *Am J Med Genet C Semin Med Genet*. 2017;175(1):8-26.
33. Parapia LA, Jackson C. Ehlers-Danlos syndrome—a historical review. *Br J Haematol*. 2008;141(1):32-35.

CME QUIZ: VOLUME 45, NUMBER 8

To earn CME credit, you must read the CME article and complete the quiz and evaluation on the enclosed answer form, answering at least seven of the 10 quiz questions correctly. **Select the best answer and use a blue or black pen to completely fill in the corresponding box on the enclosed answer form.** Please indicate any name and address changes directly on the answer form. If your name and address do not appear on the answer form, please print that information in the blank space at the top left of the page. Make a photocopy of the completed answer form for your own files and <u>mail the original answer form</u> in the enclosed postage-paid business reply envelope. Only two entries will be considered for credit. Your answer form must be received by Lippincott CME Institute, Inc., by **April 14, 2024.** For more information, call (800) 638-3030.

All CME credit earned via *Contemporary Diagnostic Radiology* will apply toward continuous certification requirements. ABR continuous certification requires 75 CME credits every 3 years, at least 25 of which must be self-assessment CME (SA-CME) credits. All SAM credits earned via *Contemporary Diagnostic Radiology* are now equivalent to SA-CME credits (www.theabr.org).

Online quiz instructions: To take the quiz online, **log on to your account at www.cdrnewsletter.com,** and click on the "CME" tab at the top of the page. Then click on "Access the CME activity for this newsletter," which will take you to the log-in page for http://cme.lww.com. Enter your **username** and **password**. Follow the instructions on the site. You may print your official certificate *immediately*. Please note: Lippincott CME Institute **will not** mail certificates to online participants. **Online quizzes expire on the due date.**

1. "Hidebound appearance" refers to
   A. asymmetric fibrosis of the antimesenteric side of the bowel wall.
   B. delayed motility resulting in fecalization of the small bowel.
   C. small bowel fibrosis with luminal dilation and longitudinal approximation of the folds of the valvulae conniventes.
   D. dilated and fluid-filled esophagus.

2. Which one of the following describes NSIP?
   A. reticular interstitial markings predominantly involving the middle lobe
   B. reticular interstitial markings predominantly involving apicoposterior segments of both upper lobes
   C. severe traction bronchiectasis
   D. ground-glass opacities with more frequent subpleural involvement and lesser prevalence of traction bronchiectasis

3. Which one of the following organisms is slightly more prevalent in patients with SLE than in the general population?
   A. *Chlamydia trachomatis*
   B. *Shigella*
   C. *Salmonella*
   D. *Nocardia*

4. In patients with SjS, the "salt and pepper" appearance of salivary glands on MRI refer to
   A. homogeneous T1 and T2.
   B. heterogeneous T1 and T2.
   C. hypointense on T1 and hyperintense on T2.
   D. hyperintense on T1 and hypointense on T2.

5. MRI findings of muscles with IBM usually are
   A. bilateral and asymmetric with marked edema.
   B. bilateral and symmetric with marked edema.
   C. unilateral with marked edema.
   D. bilateral and symmetric with volume loss and fatty infiltration.

6. The two most important organs involved in MCTD are
   A. pulmonary and MSK.
   B. cardiac and pulmonary.
   C. cardiac and MSK.
   D. cardiac and GIT.

7. Figure 11 is a spinal radiograph in a 41-year-old, HLA-B27-positive man with longstanding lower back pain. Which one of the following signs is present?
   A. Romanus lesion
   B. dagger
   C. shiny corners
   D. arachnodactyly

Figure 11.

8. Aside from PsA, arthritis mutilans can also be seen in association with
   A. AS.
   B. rheumatoid arthritis.
   C. SLE.
   D. IBM.

9. Which one of the following is the *best* modality to assess diameters of the dilated ascending aorta, sinotubular junction, and aortic root in patients with MFS?
   A. conventional radiographs
   B. sonography
   C. sonography with color Doppler
   D. CT

10. The Ehlers-Danlos syndrome subtype associated with fatal rupture of the bowels, organs, and large arteries is type
    A. I.
    B. II.
    C. III.
    D. IV.